



ELSEVIER

Available online at www.sciencedirect.com

SCIENCE @ DIRECT®

Earth and Planetary Science Letters 227 (2004) 37–56

EPSL

www.elsevier.com/locate/epsl

Genesis of the Western Samoa seamount province: age, geochemical fingerprint and tectonics

S.R. Hart^{a,*}, M. Coetzee^b, R.K. Workman^a, J. Blusztajn^a, K.T.M. Johnson^c,
J.M. Sinton^c, B. Steinberger^d, J.W. Hawkins^e

^a*Woods Hole Oceanographic Institution, Woods Hole, MA 02543, USA*

^b*University of Cape Town, Cape Town, Rondebosch, 7701, South Africa*

^c*University of Hawaii at Manoa, Honolulu, HI 96822, USA*

^d*Japan Marine Science and Technology Center, Yokosuka 237-0061, Japan*

^e*Scripps Institution of Oceanography, La Jolla, CA 92093, USA*

Received 11 March 2004; received in revised form 2 August 2004; accepted 5 August 2004

Editor: K. Farley

Abstract

The Samoan volcanic lineament has many features that are consistent with a plume-driven hotspot model, including the currently active submarine volcano Vailulu'u that anchors the eastern extremity. Proximity to the northern end of the Tonga trench, and the presence of voluminous young volcanism on what should be the oldest (~5 my) western island (Savai'i) has induced controversy regarding a simple plume/hotspot model. In an effort to further constrain this debate, we have carried out geochronological, geochemical and isotopic studies of dredge basalts from four seamounts and submarine banks that extend the Samoan lineament 1300 km further west from Savai'i. ⁴⁰Ar/³⁹Ar plateau ages from Combe and Alexa Banks (11.1 my—940 km, and 23.4 my—1690 km from Vailulu'u, respectively) fit a Pacific age progression very well. The oldest volcanism (9.8 my) on Lalla Rookh (725 km from Vailulu'u) also fits this age progression, but a new age is much younger (1.6 my). Isotopically, these three seamounts, along with Pasco Bank (590 km from Vailulu'u), all lie within, or closely along extensions of, the Sr–Nd–Pb fields for shield basalts from the Eastern Samoan Province (Savai'i to Vailulu'u); this clearly establishes a Samoan pedigree for this western extension of the Samoan hotspot chain, and pushes the inception of Samoan volcanism back to at least 23 my. From geodetic reconstructions of the Fiji–Tonga–Samoa region, we show that the northern terminus of the Tonga arc was too far west of the Samoa hotspot up until 1–2 my ago to have been a factor in its volcanism. Young rejuvenated volcanism on Lalla Rookh and Savai'i may be related to the rapid eastward encroachment of the Trench corner. The Vitiiaz Lineament,

* Corresponding author.

E-mail address: shart@whoi.edu (S.R. Hart).

previously thought to mark a proto-Tongan subduction zone, was more likely created by the eastward propagation of the tear in the Pacific Plate at the northern end of the arc.

© 2004 Elsevier B.V. All rights reserved.

Keywords: Samoa; geochemistry; tectonics; 40/39 Ar ages; Vitiaz Lineament; Tonga Trench; hotspot volcanism

1. Introduction

The question of whether the Samoan volcanic lineament is or is not a “plume-driven” age-progressive hotspot chain has been debated for decades. Hawkins and Natland [1] and Natland [2] noted that the voluminous young volcanism on Savai’i was inconsistent with a simple hotspot model, and suggested that at least some of the volcanic timing was controlled by tectonism related to proximity to the Tonga Trench, and the transform zone bounding that subduction zone on the north. Duncan [3] noted a reasonable age-progressive trend, when the ages of the seamounts to the west of Savai’i are taken into account. His argument implicitly invokes a Samoan “pedigree” for these seamounts, and the available geochemical data were consistent with this [4,5]. With the exception of Savai’i, there is a consistent east to west aging of volcano morphology, as witnessed by youthful uneroded shield morphology at Ta’u, well-advanced erosion of shield on Tutuila with the beginning of a post-erosional veneer, and a major post-erosional veneer on Upolu, covering deeply eroded shield remnants. As noted by Natland [2], any possible shield on Savai’i has been massively covered by post-erosional volcanism. While accepting a “younging to the east” model, Natland and Turner [6] were unwilling to accept this as proof of a hotspot model, arguing that the volcanism could still be driven by thermo-mechanical processes related to the corner of the Tonga Trench. Natland [7] has presented a new model for Samoa where the volcanism is all derived from shallow sources, under control of plate fracture mechanics. However, the discovery of the young active submarine volcano Vailulu’u, anchoring the eastern end of the chain, and well removed from the corner of the Tonga trench, lend strong support to a basic plume model. Furthermore, recent seismic tomography has imaged a plume stem under Samoa, extending well into the lower mantle [8]. This of course does not preclude a

strong “rejuvenated” stage of volcanism related to proximity to the northern Tonga transform zone as advocated by Hawkins and Natland [1].

The purpose of this paper is to firmly define a Samoan chemical pedigree for the WESAM (Western Samoan) seamounts, and to provide new age data relevant to the question of age progression in the WESAM province.

2. Physical setting

Conventionally, the Samoa hotspot lineament stretches from the large subaerial island of Savai’i in the west, to Ta’u Island in the east (see Fig. 1A). Vailulu’u seamount (originally discovered and named Rockne Volcano [9]) has recently been shown to be volcanically active [10], and is thought to be the current location of the Samoan hotspot. In addition, the long ridge extending SE from Tutuila has been swath-mapped, and culminates in a young volcano named Malumalu (The Cathedral). Comprehensive geochemical and isotopic data now exist for all of the volcanoes of this “Eastern Volcanic Province” [11–13,2]. West of Savai’i, there are many seamounts and submarine banks that may reflect continuation of the Samoan lineament (Fig. 1B). However, these do not define a single lineament, and it is uncertain which of these may be part of the Samoan Chain, as opposed to belonging to other older hotspot chains that may have lineaments passing through this region (for example, the Tuvalu lineament [14] or lineaments from the Cook–Austral or Louisville hotspots [15–17]).

A number of these western seamounts were dredged during the 1982 KK820316 cruise of the R/V *Kana Keoki*, and initial petrographic, geochronologic and major element analyses did support a Samoan pedigree for some of these features [3–5,18]. In addition, a nephelinite dredged from Pasco Bank during the 1971 ANTIPODE cruise was shown

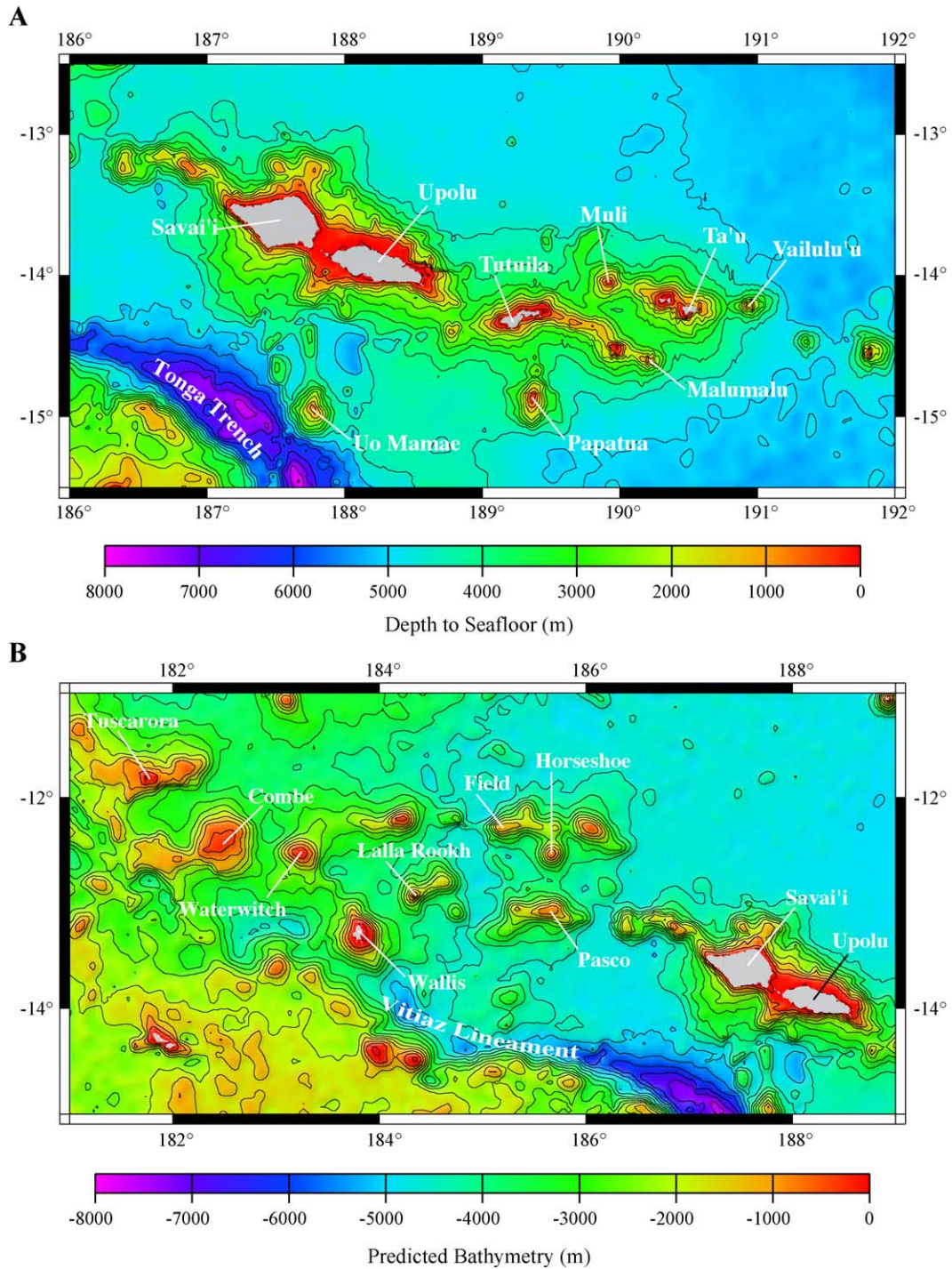


Fig. 1. (A, B) Location map for the WESAM (Western Samoa) seamounts relative to the subaerial islands (Savai'i, Upolu, Tutuila and Ta'u) and submarine volcanoes (Muli, Malumalu and Vailulu'u) of Eastern Samoa. Papatua (PPT) and Uo Mamae (Machias) are isolated seamounts that may or may not be related to the Samoa hotspot. Alexa Bank is not shown in panel B, but lies almost 7° further WNW from Combe. The Vitiiaz Lineament is shown as a continuation of the northern termination of the Tonga Trench.

Table 1
Western Samoa seamounts, dredge locations

Dredge no.	Seamount	Setting of dredge	Latitude	Longitude	Relief (top–bottom)	Dredge depth (m)	Distance from Vailulu'u (km)
239	Pasco Bank	SE flank	13.143°S	174.300°W	13–4800 m	1679–1567	579
3	Lalla Rookh Bank	S slope	12.985°S	175.635°W	18–4400 m	2800–2400	723
7	Combe Bank	SW ridge	12.702°S	177.685°W	25–3500 m	2800–2550	948
14	Alexa Bank	W ridge	11.685°S	184.953°W	180–3300 m	3500–2800	1745

239: SIO Antipode, leg 16 [1].

3, 7, 14: Cruise KK820316, leg 2, R/V Kana Keoki [4].

to be geochemically similar to Samoan basalts [1]. We have fully re-inspected the dredge collection from the Kana Keoki cruise, along with the existing thin section collection, and selected the best available material from Lalla Rookh, Combe and Alexa for further geochemical and geochronologic work. The bathymetry and dredge locations for these seamounts are given in Table 1, and more fully described in Brocher [14] and Sinton et al. [4]. The Pasco Bank setting is described in Hawkins and Natland [1].

3. Techniques

Cut slabs were rough-crushed in plastic, and the cleanest possible chips were handpicked and powdered in agate. Major and trace elements were done on these powders by combined XRF/ICP-MS at the GeoAnalytical Lab, Washington State University. Powders for isotopic analysis were leached in warm 6 N HCl for 1 h; Sr and Nd chemistry was done with conventional ion chromatography, using DOWEX 50 cation resin, and HDEHP-treated teflon for Nd separation [19]. Pb chemistry utilized the HBr–HNO₃ procedure of Galer [20] and Abouchami et al. [21], with a single column pass. Sr and Nd analyses were done on the WHOI VG354 TIMS multi-collector; these analyses carry internal precisions of 5–10 ppm; external precision, after adjusting to 0.710240 and 0.511847 for the SRM987 and La Jolla Nd standards, respectively, is estimated to be 15–25 ppm. Pb isotopic analysis was done on the WHOI NEPTUNE [64]. Pb analyses carry internal precisions on XXX/204 (where XXX=206, 207 or 208) ratios of 15–30 ppm; SRM997 Tl was used as an internal

standard, and external reproducibility (including full chemistry) ranges from 17 ppm for ²⁰⁷Pb/²⁰⁶Pb, to 117 ppm for ²⁰⁸Pb/²⁰⁴Pb [22]. Pb ratios were adjusted to the SRM981 values of Todt et al. [23]; two separate lots of the SRM981 standard were inter-compared and any possible isotopic heterogeneity between these lots was <10 ppm for XXX/204 ratios, and <1.5 ppm for ²⁰⁸Pb/²⁰⁶Pb ratios.

4. Age–distance relationships

New high quality ⁴⁰Ar/³⁹Ar step-release plateau ages for Lalla Rookh, Combe and Alexa seamounts are given in Table 2, along with earlier 40/39 total fusion ages for other samples from these same dredges [3]. Ages were measured on hand-picked holocrystalline fragments from the whole rock material. No glass was encountered during the picking, and though the dredge depths were all relatively deep (Table 1), we do not see any evidence in the 40/39 plateau data for excess argon. A summary of all Samoa age data as a function of distance from Vailulu'u is shown in Fig. 2.

For Lalla Rookh, the new age is 8 my younger than the prior age, and establishes a very long eruptive history for this seamount; while the older age is quite consistent with the expected age progression, the young age clearly is not. In this respect, it is similar to the young (0.08–0.8 my) volcanism on Wallis Island, some 70 km SW of Lalla Rookh [3,26] Unfortunately, there are no geochemical data for the old sample (3-16), to test if the large age gap is accompanied by significant geochemical differences. The young sample has similar major element characteristics to four other basalts from the same dredge [4].

Table 2
 $^{40/39}\text{Ar}$ plateau ages, Western Samoa seamounts

Sample number	Location	Steps used/ total steps	^{39}Ar fraction used	40/39 Total fusion (my)	Weighted plateau (my)
3–26	LALLA ROOKH	6/6	0–100%	1.63 ± 0.06	1.62 ± 0.05
3–16 ^a	LALLA ROOKH			9.8 ± 0.3	
7–100	COMBE	8/9	4.6–100%	11.03 ± 0.07	11.12 ± 0.06
7–11 ^a	COMBE			14.1 ± 1.1	
14–19	ALEXA	5/9	20.0–95.9%	34.01 ± 0.55	23.94 ± 0.36
14–100	ALEXA	4/8	8.2–67.4%	27.80 ± 0.24	22.91 ± 0.20
14–23 ^a	ALEXA			36.9 ± 0.5	

• Step-release heating from 600 to 1400 °C.

• 2σ errors include measurement uncertainties, and uncertainty in J -value (flux gradient from FCT-3 biotite monitor), but not uncertainty in monitor age.

• New ages are from the lab of Robert A. Duncan, Oregon State University (full details may be found in Supplementary materials).

^a These samples were reported by Duncan [3].

For Combe, the new age is in reasonable agreement with the earlier data (11.1 versus 14.1 my), and together they straddle the expected age line.

For Alexa bank, the two new ages agree very well (22.9 and 23.9 my), though the total fusion ages are significantly older (as was the total fusion age of 36.9 my reported by Duncan [3]). This appears to remove the inconsistency in the older data with respect to the age progression; the two new ages fall very close to the 7.1 cm/year age progression (Fig. 2).

In summary, insofar as Lalla Rookh, Combe and Alexa can be shown to be of Samoan pedigree (see below), the new data for Combe and Alexa strongly support a simple age-progressive nature for the Samoan lineament. At the same time, the young age for Lalla Rookh (and Wallis) provides evidence for a late stage of rejuvenation, perhaps related to tectonism along the northern Tongan transform zone, as advocated by Hawkins and Natland [1], and Natland and Turner [6].

5. Geochemical characteristics

5.1. Alteration effects

Given that all of the WESAM basalts are submarine dredge samples, and exposed to seawater for times up to 24 my, the likelihood of weathering and alteration effects must be considered. The alkalis are among the most mobile elements under

these conditions [27], so that ratios such as Rb/Cs and Rb/Ba may be used as “alteration indicators”. Fig. 3 compares these ratios in WESAM basalts with values from both submarine and subaerial Samoan volcanoes, and with the “canonical” values established for fresh oceanic basalts by Hofmann and White [28], the 2σ bounds of which are shown in Fig. 3 by the rectangle. Only four of the WESAM samples fall within the field of other (younger and fresher?) Samoan basalts, and only three fall close to the canonical field; the remainder are well outside the rectangle and the Samoan field. Submarine weathering typically involves addition of alkalis, in the order $\text{Cs} > \text{Rb} > \text{K}$; Ba is less mobile and more erratic [27,29]. This would cause trajectories down and to the right in Fig. 3 (note “submarine” arrow); only two WESAM samples have moved in that direction. Subaerial basalt weathering typically leads to leaching of alkalis [30], though the relative leaching behavior of Rb and Cs has not been established (note “subaerial” arrow). Curiously, seven of the WESAM samples are in fact closely aligned along a Rb-mobility trajectory (solid line in Fig. 3); four of the samples exhibit marked Rb depletion. Location along this line implies a constant Ba/Cs ratio during alteration, and we know of no reason why Rb would be mobile and not Cs. Comparing data for 58 subaerial and 38 submarine basalts from the Eastern Volcanic Province [11] shows no statistically significant difference between basalts erupted above water or underwater ($\text{Rb}/\text{Cs} = 96 \pm 9$ and 117 ± 12 ; Rb/

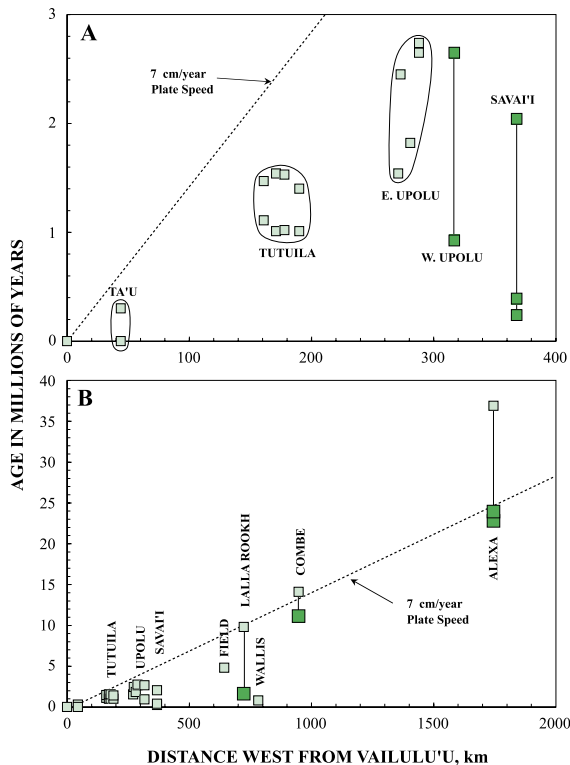


Fig. 2. (A) Age–Distance relationships for “shield” lavas from the subaerial Samoan islands. Ta’u, Tutuila and Eastern Upolu data (small lightly shaded squares) are K–Ar ages, from McDougall [24] and Natland and Turner [6]. The Tutuila field shows the range of data available, not all of the individual ages. Western Upolu and Savai’i data (large darkly shaded squares) are $^{40}/^{39}$ Ar plateau ages [11]. (B) Age–Distance relationships for dredge basalts from the WESAM Seamount province (the subaerial data from panel A is also shown, small filled squares). Small lightly shaded squares are $^{40}/^{39}$ Ar total fusion ages, from Duncan [3]; large darkly shaded squares are $^{40}/^{39}$ Ar “plateau” ages, from Table 2. The dashed line is for the 7 cm/year local Pacific plate velocity derived from the REVEL and NUVEL-1A plate models [25].

Ba=0.117±0.006 and 0.105±0.007, submarine versus subaerial, respectively, 2 σ standard errors). We have no ready explanation for the type of mobility expressed in the WESAM basalts; though the tops of these seamounts were certainly subaerially exposed in their younger days, the samples were dredged from depths well-below possible subaerial exposure (Table 1).

In any event, the alkalis in the WESAM samples have clearly been mobile, and this suggests caution in using the alkali data, or that for other potentially

mobile elements such as U. Since Th is generally insensitive to alteration, and Th/U is a relatively constant ratio in OIBs, this ratio can provide added information about the trace element reliability in the WESAM basalts. U behaves much like the alkalis during weathering, being added in submarine domains [31] and leached in subaerial domains. Surprisingly, the four samples from the oldest seamount, Alexa, have normal and nearly constant Th/U (3.50–3.76, Table 3). One sample from Lalla Rookh has very high Th/U (8.9; sample 3-43), and one from Combe is very low (2.1; sample 7-100); the other samples from these seamounts are normal. This suggests that spidergram patterns will in general be useful for petrogenetic considerations.

The isotope data appear quite robust with respect to alteration effects (note that this may in part be due to the strong leaching that sample powders undergo prior to analysis). Again, the four samples from the oldest seamount, Alexa, while wildly dispersed in the Rb/

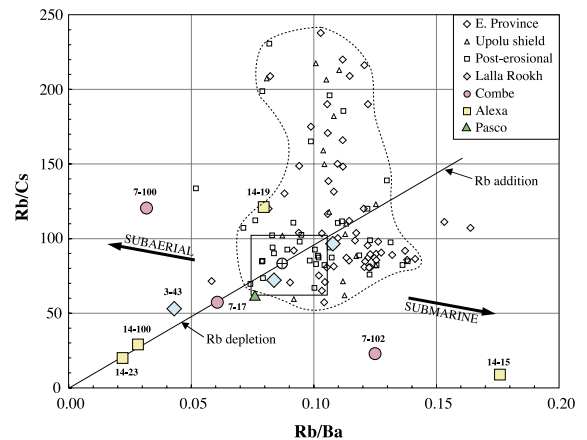


Fig. 3. Rb/Cs–Rb/Ba relationships of WESAM basalts, in comparison to other Samoan basalts. The field encloses both shield and post-erosional basalts from Vailulu’u, Ta’u, Muli, Malumalu and Upolu, and post-erosional basalts from Upolu and Savai’i (four widely scattered point are not enclosed; data from Workman et al. [11]). The rectangle represents ± 2 standard deviations from the mean (circled cross) of the canonical Rb/Ba and Rb/Cs values recommended for oceanic basalts by Hofmann and White [28]. The arrows represent general tendencies for subaerial and submarine weathering (see text). The solid line represents a Rb-“mobility” trajectory, drawn through the canonical value. Note that only four of the WESAM basalts fall in the Samoan field (3-26, 3-36, 14-19, 239-1) and close to the canonical field; seven lie close to the Rb mobility line.

Table 3
Geochemical data for Western Samoa Seamounts

Sample	Pasco ^a	Lalla Rookh			Combe			Alexa			
	ANT 239-1	3-26	3-36	3-43	7-17	7-100	7-102	14-15	14-19	14-23	14-100
SiO ₂	39.75	41.61	42.93	48.33	46.62	45.56	46.96	50.03	50.15	48.82	49.07
Al ₂ O ₃	12.61	10.66	11.37	15.14	13.25	13.78	13.57	14.40	14.57	14.87	14.92
TiO ₂	3.77	3.855	4.332	4.023	3.759	3.880	4.020	2.712	2.934	3.084	3.224
FeO*	12.19	13.49	13.66	11.39	13.71	14.18	12.14	11.34	12.74	12.47	12.36
MnO	0.15	0.193	0.185	0.129	0.305	0.220	0.169	0.139	0.151	0.274	0.341
MgO	11.95	12.67	9.58	5.75	6.96	6.00	8.93	6.84	6.61	6.95	6.56
CaO	13.97	11.13	12.58	9.46	10.08	12.10	8.18	10.66	8.98	8.80	8.79
Na ₂ O	2.64	3.129	2.627	3.384	3.103	2.716	3.816	2.911	3.033	3.915	3.832
K ₂ O	1.82	2.636	2.008	1.543	1.433	0.754	1.728	0.675	0.538	0.436	0.518
P ₂ O ₅	1.14	0.638	0.729	0.850	0.783	0.805	0.490	0.293	0.298	0.371	0.387
Pre-total	95.88	99.40	98.60	97.23	97.01	96.82	97.22	99.27	98.57	98.58	98.38
Mg#	0.673	0.663	0.595	0.514	0.516	0.470	0.607	0.559	0.521	0.539	0.527
Ni	280	265	246	69	319	171	248	65	52	96	98
Cr	463	373	373	74	502	586	270	103	32	142	129
V	250	292	344	303	356	356	302	318	349	333	347
Ga		20	20	24	23	21	17	25	22	20	21
Cu	65	59	114	64	101	148	92	117	78	92	96
Zn	150	131	136	162	136	123	115	103	123	92	84
Cs	0.802	0.795	0.702	0.406	0.221	0.043	1.208	2.068	0.056	0.143	0.124
Rb	48.7	76.2	50.6	21.50	12.68	5.21	27.70	18.08	6.79	2.86	3.61
Ba	644	707	604	499	209.1	164.2	221.7	102.8	85.3	129.9	127.5
Th	6.49	6.01	7.92	10.22	2.562	2.574	3.087	1.468	1.398	1.930	1.940
U	1.106	1.207	1.606	1.150	0.617	1.233	0.725	0.420	0.372	0.538	0.534
Nb	83.9	65.9	87.6	72.5	28.92	30.76	35.8	16.67	15.36	20.66	20.35
Ta	5.16	4.42	5.68	4.90	2.084	2.205	2.547	1.184	1.094	1.439	1.443
La	70.3	43.5	66.7	65.2	24.16	26.51	28.54	14.16	12.59	18.25	17.56
Ce	132.1	77.5	123.2	117.0	51.4	51.1	61.7	33.10	27.66	40.4	38.9
Pb	5.42	5.67	4.78	6.29	6.69	2.822	2.931	1.485	1.281	0.957	0.763
Pr	15.98	8.74	13.74	13.53	6.56	7.31	7.79	4.37	3.67	5.25	5.06
Nd	62.5	36.1	55.3	54.4	30.3	33.5	34.6	20.65	17.42	24.41	23.07
Sr	739	663	794	817	406	473	628	346	316	360	359
Zr	252.5	173.9	263.0	300.5	203.9	213.6	236.1	158.8	150.1	179.8	177.2
Hf	5.75	4.75	6.84	7.98	5.47	5.55	6.13	4.30	4.08	4.72	4.74
Sm	12.55	8.39	11.61	11.94	8.27	8.98	8.84	5.82	5.08	6.69	6.42
Eu	3.534	2.722	3.64	3.76	2.599	2.942	2.824	2.099	1.986	2.339	2.301
Gd	10.25	7.40	9.93	10.21	8.10	8.62	8.27	6.25	5.52	6.91	6.59
Tb	1.313	1.121	1.369	1.445	1.253	1.322	1.247	1.008	0.940	1.097	1.064
Dy	6.52	5.79	7.05	7.66	6.97	7.20	6.81	5.89	5.61	6.30	6.17
Ho	1.083	0.977	1.199	1.320	1.258	1.295	1.237	1.093	1.074	1.174	1.150
Y	34.20	25.12	30.06	37.16	32.13	33.20	31.14	27.88	26.99	30.01	29.77
Er	2.533	2.150	2.655	3.132	3.001	3.097	2.916	2.687	2.643	2.894	2.857
Tm	0.316	0.254	0.329	0.391	0.394	0.401	0.384	0.363	0.370	0.387	0.384
Yb	1.759	1.326	1.741	2.145	2.199	2.209	2.169	2.105	2.128	2.232	2.203
Lu	0.254	0.173	0.249	0.306	0.318	0.318	0.300	0.304	0.327	0.319	0.327
Sc	24.92	20.79	26.72	20.48	28.35	35.74	25.88	35.33	33.52	30.82	29.18
⁸⁷ Sr/ ⁸⁶ Sr	0.705916	0.704430	0.704467	0.704931	0.704828	0.704698	0.704816	0.703489	0.703498	0.703591	0.703622
¹⁴³ Nd/ ¹⁴⁴ Nd	0.512715	0.512795	0.512802	0.512812	0.512855	0.512819	0.512823	0.512964	0.512945	0.512920	0.512921
²⁰⁶ Pb/ ²⁰⁴ Pb	18.9479	19.1674	19.6570	19.2688	18.9591	19.1730	18.9724	18.7431	18.7171	18.7727	18.7763
²⁰⁷ Pb/ ²⁰⁴ Pb	15.5978	15.6189	15.6252	15.6143	15.5857	15.5878	15.5760	15.5273	15.5189	15.5302	15.5387
²⁰⁸ Pb/ ²⁰⁴ Pb	39.2874	39.2042	40.0460	39.6267	39.0212	39.2519	39.0617	38.5409	38.4937	38.5771	38.5876

Major elements are calculated volatile-free; pre-total without volatiles; Mg# is calculated with FeO=0.85 FeO*.

^a Major element data for 239-1 is from Hawkins and Natland [1].

Cs–Rb/Ba plot, are virtually constant in ⁸⁷Sr/⁸⁶Sr, with a maximum spread of only 0.02%; the same is true of Combe. As Nd and Pb are generally less

affected by weathering and alteration than Sr, we argue that all of the isotope data are reliable for the purposes of establishing a Samoan signature.

5.2. Classification and major elements

The alkali–silica–MgO variations are shown in Fig. 4A,B. The single sample from Pasco Bank is a nephelinite [1], and the most under-saturated of the whole WESAM sample suite. The Lalla Rookh

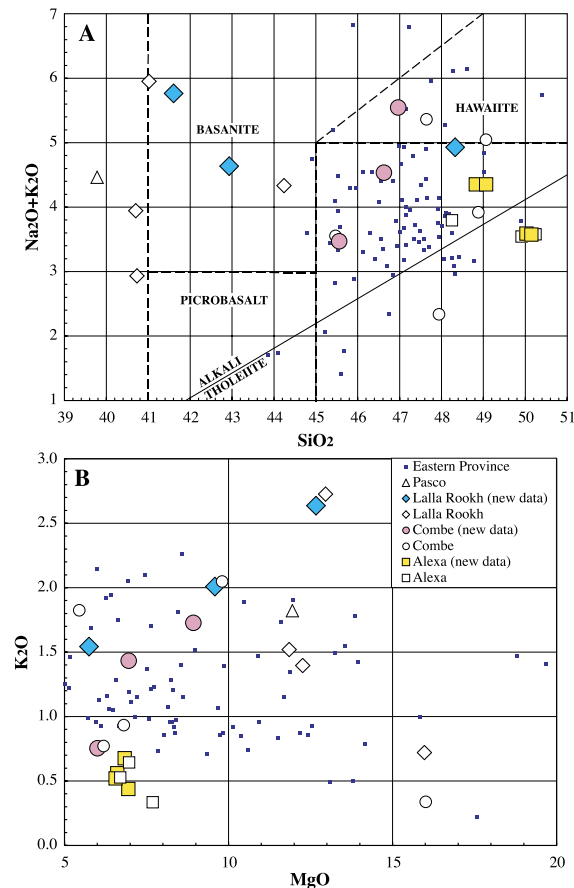


Fig. 4. (A) Alkali–silica classification plot for new basalt data (shaded symbols) from Pasco, Lalla Rookh, Combe and Alexa seamounts (see legend in panel B). For comparison, data for other samples from three of the same dredges are shown as unfilled symbols [4], and all available data for Eastern Province basalts is shown as small dots [2,11]. Note that our three Lalla Rookh samples (shaded diamonds) are portions of the same three rocks reported by Sinton et al. [4]; other than this, there is no overlap between the sample suites. The alkali basalt/tholeiite dividing line is that of Macdonald and Katsura [32]. The Eastern Province samples that plot in the tholeiite field with less than 47% silica are all strongly picritic. Dashed lines indicate the basalt classification of Le Bas et al. [33]. (B) K_2O –MgO variation diagram for basalts from the WESAM and Eastern Province, as described in A. The high MgO samples are all either picritic or ankaramitic.

samples vary widely in composition, ranging from undersaturated high-alkali basanites (3-26) to moderately differentiated alkali basalt (3-43). Three samples analyzed by Sinton et al. [4] from the same dredge are ankaramitic basanites; a fourth is a basanite similar to our sample 3-26. Note that this most alkalic sample is the one with the young plateau age (1.62 my); the sample dated at 9.8 my by Duncan [3] was not analyzed for major elements, but its K_2O content (1.2%) is clearly lower than that of sample 3-26, possibly suggesting a typical (for Samoa) early alkali basalt shield-building stage, followed after a long hiatus by a highly undersaturated “rejuvenated” stage.

Our Combe samples are alkali basalts, though one is differentiated and slightly hawaiitic. They continue the unusual positive trend on the K_2O –MgO plot (Fig. 4B) defined by our Lalla Rookh samples. They tend to be more alkalic than the Sinton et al. samples from the same dredge; one of these latter (7-11) was classified as tholeiitic, but we believe this is a cpx accumulation signature, and that this sample is innately alkalic, like our (aphyric) samples. While we do not have cpx analyses for any of these rocks, phenocrysts from several E. Province basalts have very low $\text{Na}_2\text{O}+\text{K}_2\text{O}$ (<0.5%), and would pull whole rock compositions into the tholeiitic field. At face value, the total fusion age for the 7-11 “tholeiite” is older than our plateau age on 7-100 (14.1 versus 11.1 my), but we do not feel this represents a Hawaiian-type “age transition” from tholeiite to alkali basalt.

Our four Alexa samples are all very similar in major elements, and straddle the alkali basalt–tholeiite dividing line; they are also all relatively low in MgO. The two tholeiitic samples have the same low MgO as the others, so have not simply been pulled into the tholeiitic field by cpx accumulation. Three of our Alexa samples are cut from the same samples as those analyzed by Sinton et al. [4], and agree very well in composition.

The data for these WESAM province basalts can be compared in Fig. 4 to data from both subaerial and submarine samples from the Eastern Volcanic Province (EVP) of Samoa (small filled symbols); only the Pasco and Lalla Rookh samples plot well outside the field of these EVP basalts. While the Alexa tholeiites appear to be higher in SiO_2 than most of the EVP tholeiites, it should be noted that many of these latter tholeiites, especially those that are low in SiO_2 , are

strongly picritic; in aphyric “state” they would plot much closer to the Alexa tholeiites.

5.3. Isotopic signatures

It is well established that Samoan volcanism is of EM2 character, and indeed is the most extreme example of EM2, with $^{87}\text{Sr}/^{86}\text{Sr}$ values as high as 0.7089 [10,11]. In Sr–Nd–Pb isotope “space”, Samoa occupies a unique domain relative to other mantle end-members [34] and all other oceanic island basalts (OIBs). It is even distinctive relative to the Society hotspot, which is also strongly EM2 in character. For example, Workman et al. [11] show that every analyzed Samoan basalt has a higher $\Delta^{87/4}\text{Pb}$ [35] than any basalt from the Society hotspot. Isotopic fingerprints then should allow us to ascertain the “pedigree” of the WESAM seamounts with some certainty.

The WESAM isotope data are compared with fields for the subaerial and submarine volcanoes of Samoa in Fig. 5. Note first that post-erosional and shield basalts in Samoa are isotopically distinct from each other, as first pointed out by Wright and White [12]; the PE basalts are consistently lower in $^{206}\text{Pb}/^{204}\text{Pb}$. The nephelinite from Pasco Bank appears to be transitional between shield and PE, in terms of Sr and Pb isotopes. None of the other WESAM samples show any PE tendencies in this isotope space. It is difficult to say whether this argues against a rejuvenated stage of volcanism in the WESAM province, or is just a reflection of sampling limitations; we are dealing here with samples from only one dredge for each of the four WESAM seamounts.

In Sr and Pb isotopes, the four basalts from Alexa are very tightly clustered. Two of the three Combe basalts are similar, whereas a third sample resembles sample 3-26 from Lalla Rookh in having higher $^{206}\text{Pb}/^{204}\text{Pb}$. The Lalla Rookh samples show a limited range in Sr and Nd ratios, but are quite variable in Pb, with sample 3-36 having the highest $^{206}\text{Pb}/^{204}\text{Pb}$ yet found for Samoan basalts. In the Sr–Pb plot (Fig. 5A), this sample and all of the Alexa samples fall outside any of the Samoan basalt fields, and on this basis might be argued to be “non-Samoan”. However, in the Pb–Pb plots (Fig. 5B,C), all of these samples are on extensions of the tightly aligned Samoan shield arrays. The Alexa samples are very close to the Upolu and Tutuila Pago shield array, while the Combe

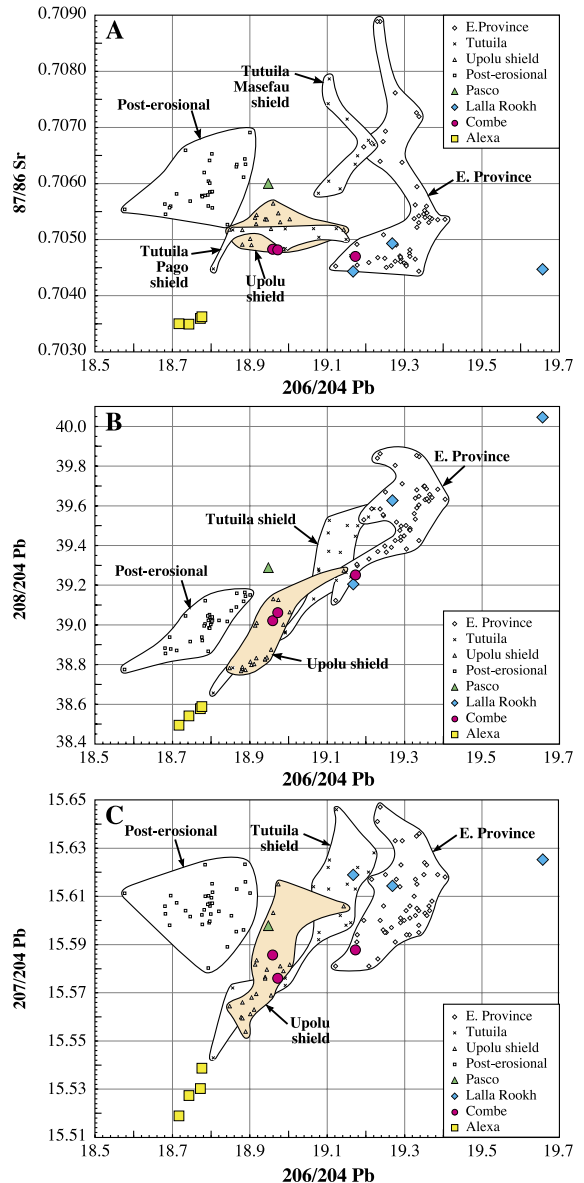


Fig. 5. $^{87}\text{Sr}/^{86}\text{Sr}$ – $^{206}\text{Pb}/^{204}\text{Pb}$ – $^{207}\text{Pb}/^{204}\text{Pb}$ – $^{208}\text{Pb}/^{204}\text{Pb}$ plot for the WESAM seamounts, in comparison with Samoa shield and post-erosional basalts. The Samoa data are divided into an Eastern Province (Ta’u Island and Vailulu’u, Muli, and Malumalu seamounts, all shield lavas [10–12]), Tutuila shields (southern and younger Pago shield, and northern, older Masefau shield [12,11]), the Upolu shield (both eastern and western shields [12,11]), and post-erosional basalts from both Upolu and Savai’i [12,11]. The WESAM seamounts appear closely affiliated with Samoa (and very distinct from fields for EM1 and HIMU basalts [34], not shown).

samples and two of the three Lalla Rookh samples are within the Samoan shield arrays. In general terms, the Samoan shield isotope data require at least three “mixing” components. Workman et al. [11] argued for four: a strongly enriched, high $^{87}\text{Sr}/^{86}\text{Sr}$ end-member (EM2), a depleted low $^{87}\text{Sr}/^{86}\text{Sr}$ –low $^{206}\text{Pb}/^{204}\text{Pb}$ component (MORB mantle?), a high ^3He component (FOZO), and a radiogenic Pb component (mild HIMU). The PE lavas, with their high $\Delta^{7/4}\text{Pb}$, require yet one more component, probably “sedimentary” in character. In this context, the isotopic signature of the WESAM basalts is easily identifiable as Samoan in general character. The Alexa basalts are extended beyond the Samoan arrays precisely in the direction of NMORB (upper) mantle, while the high $^{206}\text{Pb}/^{204}\text{Pb}$ sample from Lalla Rookh is extended toward HIMU. The remaining WESAM samples fall within the confines of the existing Samoa data. The principal characteristic of the WESAM data, vis-à-vis eastern Samoa, is the general paucity of the enriched (high

$^{87}\text{Sr}/^{86}\text{Sr}$) component; the highest $^{87}\text{Sr}/^{86}\text{Sr}$ value is 0.7049 (Lalla Rookh 3-43). While this may be just a reflection of the small sample set here, Ta’u Island, in the Eastern Province, is similarly restricted in its evidence for the enriched component (total range for Ta’u basalts is 0.7044–0.7051). We conclude that the WESAM basalts are indeed of Samoan pedigree, differing only in the somewhat larger range of $^{206}\text{Pb}/^{204}\text{Pb}$, and the relative absence of the high $^{87}\text{Sr}/^{86}\text{Sr}$ enriched component. These differences are not unexpected in what is obviously a heterogeneous mantle source and considering the much larger age range embraced by the WESAM seamounts (22 my versus only 3 my for the EVP).

5.4. Trace element signatures

The WESAM basalts can be similarly “fingerprinted” with trace elements. Based on Workman et al. [11], we have chosen a plot of Ba/Nb–Zr/Hf, Fig. 6,

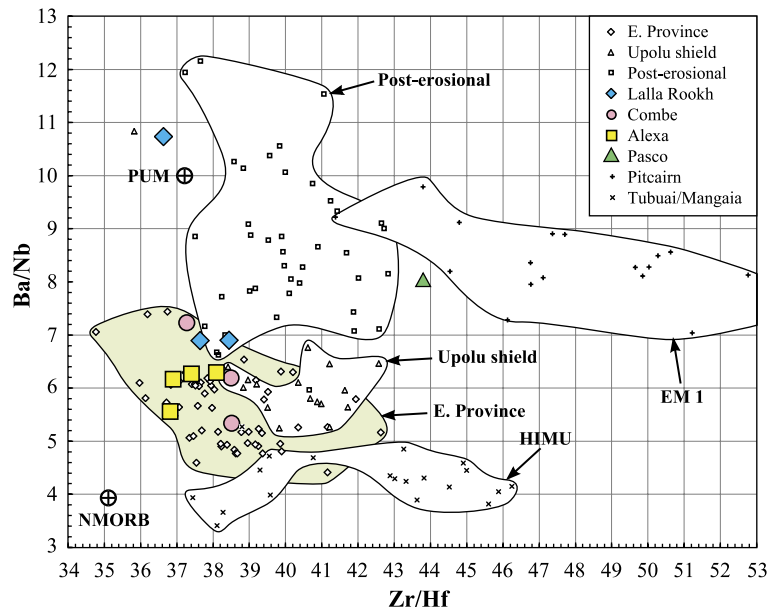


Fig. 6. Ba/Nb–Zr/Hf plot for the WESAM seamounts, in comparison with data for Samoan shield and post-erosional basalts, and end-member EM1 (Pitcairn) and HIMU (Tubuai and Mangaia) OIBs. The Pitcairn (EM1) data include both the Tedside (shield) series on the island, as well as samples from the seamounts east of the island [36–38]. Two Pitcairn samples, with Zr/Hf of 56.7 and 65.1, have been omitted from this plot. The HIMU data are from Tubuai and Mangaia Islands (Cook–Austral chain [39–41]). Average N-MORB [42] and PUM (primitive upper mantle; [43]) are also shown. Note the clear distinction between shield and post-erosional basalts from Samoa, and the distinction between the Samoan (EM2) basalts and the EM1 and HIMU fields. One Upolu sample (Ba/Nb~11.4), collected from the western (A’ana) shield, plots well outside the “shield” field on this plot, but is consistent with Upolu shield Pb data (Fig. 5). Again, the WESAM seamounts show clear kinship with Samoa.

as usefully distinguishing between Samoa and EM1 and HIMU basalts. This plot contrasts the slope of the left, more incompatible, end of a spidergram (see Fig. 7) with that of the right, less incompatible, end. Relative to the location of bulk earth (PUM), virtually all of the OIBs on this plot have positive (depleted) slopes for the left side of the spidergram, and negative (enriched) slopes for the right side of the spidergram (this “humped” shape spidergram is quite evident in Fig. 7, see below). Fig. 6 also cleanly separates Samoan shield and PE basalts, while showing little distinction between the Upolu shield, and shields of the Eastern Province. Relative to Samoa, the basalts from Pitcairn (EM1) are higher in Zr/Hf, while those from Mangaia and Tubuai (HIMU) are lower in Ba/Nb; in this plot, there is relatively little overlap between Samoa and the OIBs from end-member EM1 and HIMU.

With only two exceptions, all of the WESAM basalts are tightly clustered and plot within the field

for Eastern Province Samoan shield basalts. The exceptions are samples 239-1 from Pasco and 3-26 from Lalla Rookh, which plot close to the Samoa PE field. Both of these samples are under-saturated basanites that plot as extremes in the alkali–silica plot (Fig. 4A). Sample 3-26 has a $^{40}\text{Ar}/^{39}\text{Ar}$ age of 1.6 my, which is significantly younger than the ~10 my age expected from plate motion considerations, and might suggest a younger rejuvenated stage of volcanism on Lalla Rookh (though, as discussed above, this sample was well within the shield basalt fields on the Sr–Pb isotope plots).

The trace element patterns (spidergrams) for the averaged Lalla Rookh, Combe and Alexa data are compared to each other, and to average Ta’u Island basalt, in Fig. 7. In trace elements, Ta’u is typical of the Eastern Province basalts [11]; we use it here because it has Sr and Nd isotopic signatures most like the WESAM seamounts. In concert with their major element characteristics, which range from basanites

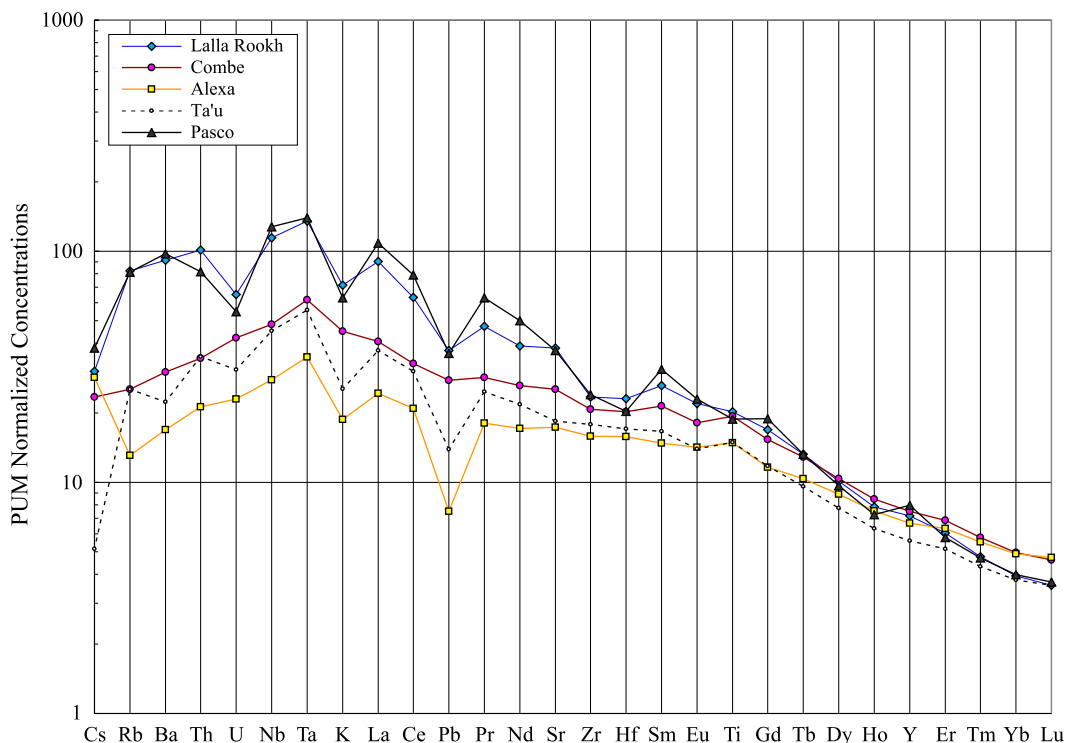


Fig. 7. Trace element patterns (spidergrams) for WESAM basalts, normalized to primitive mantle. Each location is the average of the data given in Table 3 for that location. Also shown for comparison is an average of 23 subaerial and submarine basalts from Ta’u Island, corrected to Mg# 73 by olivine addition [11]. Note that negative anomalies at U, K and Pb are typical of almost all OIB; the lack of a U anomaly for Combe and Alexa may represent addition of U during seawater interaction.

to tholeiites (Fig. 4A), Lalla Rookh has the most enriched spidergram and Alexa the least enriched. The Combe pattern is curiously smooth, without the negative U, K and Pb anomalies shared by Lalla Rookh and Ta'u; Alexa shows the K and Pb anomalies, but not the U. The negative K anomalies are not related to lithospheric interactions, as argued more generally for OIBs [65], as virtually every Eastern Province basalt, including those with high $^3\text{He}/^4\text{He}$, show the same anomaly [11]. Since these are all elements that are potentially mobile during alteration, some caution must underpin these comparisons. Note also the presence of a small negative Ba anomaly in the Ta'u pattern (and indeed in virtually every basalt from Vailulu'u and Malumalu as well), compared to all of the WESAM basalts. It seems unlikely that this is an alteration effect, unless alteration has coincidentally stopped just short of generating any hint of a positive Ba anomaly.

5.5. Pb isotope versus distance correlations

Because the Eastern Province shield basalts form a very regular increasing $^{206}\text{Pb}/^{204}\text{Pb}$ trend with distance (younging) to the east [22,11], it is useful to compare the WESAM basalts to this trend, Fig. 8.

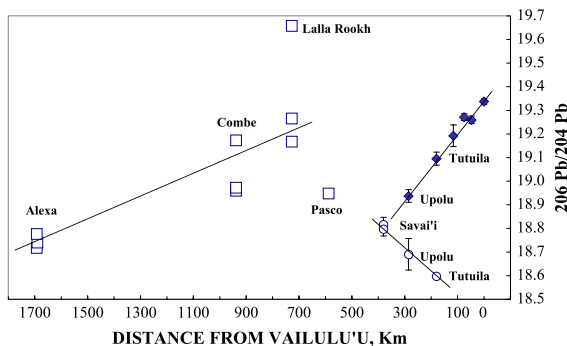


Fig. 8. $^{206}\text{Pb}/^{204}\text{Pb}$ of Samoan basalts as a function of distance from Vailulu'u volcano (the presumed present location of the Samoa hotspot). Shield basalts from the Eastern Province are shown as solid diamonds; the error bars represent 2σ standard errors for the data set given in Ref. [11]. The open circles are for post-erosional basalts from Savai'i, Upolu and Tutuila; the error bars are as above. Note that only one analysis of a PE basalt from Tutuila exists, and that all of the Savai'i data are classified as PE despite many samples analyzed from areas mapped as shield [11]. The open squares are the individual analyses from Table 3, this paper. For reference, at the accepted Pacific Plate motion velocity of 71.3 mm/year, the "age" at Pasco would be 8.2 my.

With the exception of the Pasco sample, the other three localities do show increasing $^{206}\text{Pb}/^{204}\text{Pb}$ to the east, though with considerable scatter. Pasco may represent a "resetting" of this trend, or it may provide an early start of the post-erosional trend shown in the eastern volcanoes. Note that PE basalts from Tutuila, Upolu and Savai'i form an array almost orthogonal to the shield array, and Pasco would lie near an extension of this array. We showed earlier that in Pb isotope space, Pasco was transitional between the shield and PE fields (Fig. 5); it also lies near the post-erosional field on the trace element discriminant diagram, Fig. 6. The expected age of ~8 my for Pasco is also the time when the Samoa plume may have changed its "drift" direction (see below), and this could drive a different "sampling mix" from what is clearly an isotopically heterogeneous plume.

6. Tectonic setting during WESAM province time

6.1. Regional plate motions

Because of the controversy regarding possible plume–trench interactions at present, we show in Fig. 9 our best estimate of the tectonic situation during the time of volcanic activity in the WESAM Province. Because of the enormous present-day complexity in this area, plate reconstructions in past times give only qualitative information [44,45]. Consequently, we have relied on published geodetic measurements to backtrack several key features, such as the Tonga Arc, the Fiji Platform and the Samoa Chain. Plate motion models (e.g. NUVEL-1) over time scales of 2–3 million years have been shown to be in excellent agreement [46] with current geodetic motions for the major plates in this region (Pacific and Australia). On the other hand, it is unlikely that the geodetically determined motion of sub-domains (the Tonga Arc, for example) can be confidently projected very far back in time. Zellmer and Taylor [47] have shown a persistence of Australia–Tonga vectors back to at least 0.8 my, but there are also indications that the opening rate of the northern Lau basin may have slowed significantly during subduction ~4 to ~2 my ago of the Louisville Seamount Chain (LSC; [17]). A summary of the geodetic data used in Fig. 9 is given in Table 4.

Currently, the Pacific Plate is moving N63W at 71 mm/year; the Australian Plate, New Caledonia and the Fiji Platform are all moving ~N30E, but at different rates (Australia and New Caledonia are converging on Fiji); see Fig. 9B. The three stations on the Fiji Platform are moving coherently, within the errors of the GPS survey [49]. The Tonga Arc is rotating rapidly to the east [49,63], with the transcurrent motion between Tonga and the Pacific Plate occurring somewhere in the vicinity of the Vitiaz Lineament. Various Samoan hotspot features, including Savai'i (S) and Upolu (U), are located on the Pacific Plate north of the Vitiaz. Rotuma Island (R) and Futuna-Nui Island (F; not to be confused with Futuna-Iti in Vanuatu) lie ~50 km and ~150 km south, respectively, of the Vitiaz, but are currently moving with the Pacific Plate [48]. The locus of the northern terminus of the Tonga Arc (NT), as imprinted on the Pacific Plate over the age span 4 my to present, is shown in Fig. 9B as a dotted line.

Going back in time, Fig. 9C and D, the Fiji Platform has shifted mildly to the SW, and the Samoan volcanoes have shifted markedly eastwards. The Tonga Arc rotates back to the west, docking with the Lau Ridge (an extinct arc) at ~4 my. Note that this “docking” age is somewhat younger than that constrained by geological evidence, as the initial rifting of the Lau Basin was underway at ~6.5 my, and fully active seafloor spreading was underway by 4.5 my [50]. This discrepancy likely arises from our extrapolation of current Tonga arc geodetic motions back in time as being constant; if the rate between 5 and 3 my was taken as half of current rates, the docking would occur at ~5 my, in better agreement with the geologic evidence. As noted above, the northern Lau Basin opening may also have slowed during the encounter of the LSC with the northern Tonga subduction zone. An increase of “docking” age only shifts the docking location further west (due to Fiji–Lau Ridge motion to the SW), and exacerbates the problem with the Vitiaz lineament, to be discussed below.

The “back-tracked” northern terminus (NT) of the Tonga arc (Fig. 9) passes very close to Futuna Island at 2 my, and to Rotuma Island at 4 my. A single K–Ar age of 4.9 my has been published for Futuna Island [3], so it apparently existed prior to the “drive-by” of the Tonga arc. Tholeiites from Futuna may have arc-

like chemistry [4]; if substantiated, this would be consistent with their formation above a south-dipping Vitiaz arc (now “fossil arc”). This would require that Futuna has been transferred to the Pacific plate within the past several million years. The inception age of Rotuma Island is unknown; it does exhibit <1 my rejuvenated volcanism [26], but with no arc-like geochemical characteristics.

This reconstruction appears to us to reveal several infidelities in current models for this region. First, the Vitiaz Lineament has been accepted as a proto-Tongan or “fossil” subduction zone, marking Pacific–Australian convergence prior to the inception (>7 my) of New Hebrides subduction and opening of the Lau Basin [51, 44]. However, a comparison of Fig. 9A and D shows that the Vitiaz Lineament is already well east of the early Tonga subduction zone when Tonga “undocks” from the Lau Ridge, and thus it cannot represent a fossil subduction signature from pre-Tongan subduction (though the segment west of 180 °W can be smoothly connected to the Tonga arc at 4–5 my, Fig. 9D, and thus this Vitiaz segment is consistent with identification as a “fossil” arc). On the other hand, the Vitiaz segment east of 180° closely mimics the trace of the northern terminus of the Tonga Arc as it sweeps eastward (compare Fig. 9A and B), and we propose that this is not a fossil subduction zone but rather marks the locus of the hinge of Pacific Plate tearing over the past 4–5 my. This would be consistent with the plate-bending model of Hawkins and Natland [1], for the interaction between the Pacific Plate and the Tonga subduction zone. Clear seismic evidence exists for present-day tearing at the northern terminus of the Tonga Arc [52], and the bathymetry in this area is not dissimilar to that marking the contiguous Vitiaz Lineament to the west.

The second problem concerns the NE motion of the Fiji Platform and the “wedge” of Australian Plate between the Conway–Kandavu Lineament (CKL in Fig. 9A; also called Hunter fracture zone) and the Lau Ridge. This NE motion requires convergence with the Pacific Plate, yet no obvious convergence zone has ever been delineated in the North Fiji Basin, or anywhere in the region between the Fiji Platform and the Vitiaz Lineament (now attached to the Pacific Plate). There is copious evidence for divergent motions (small spreading centers) through-

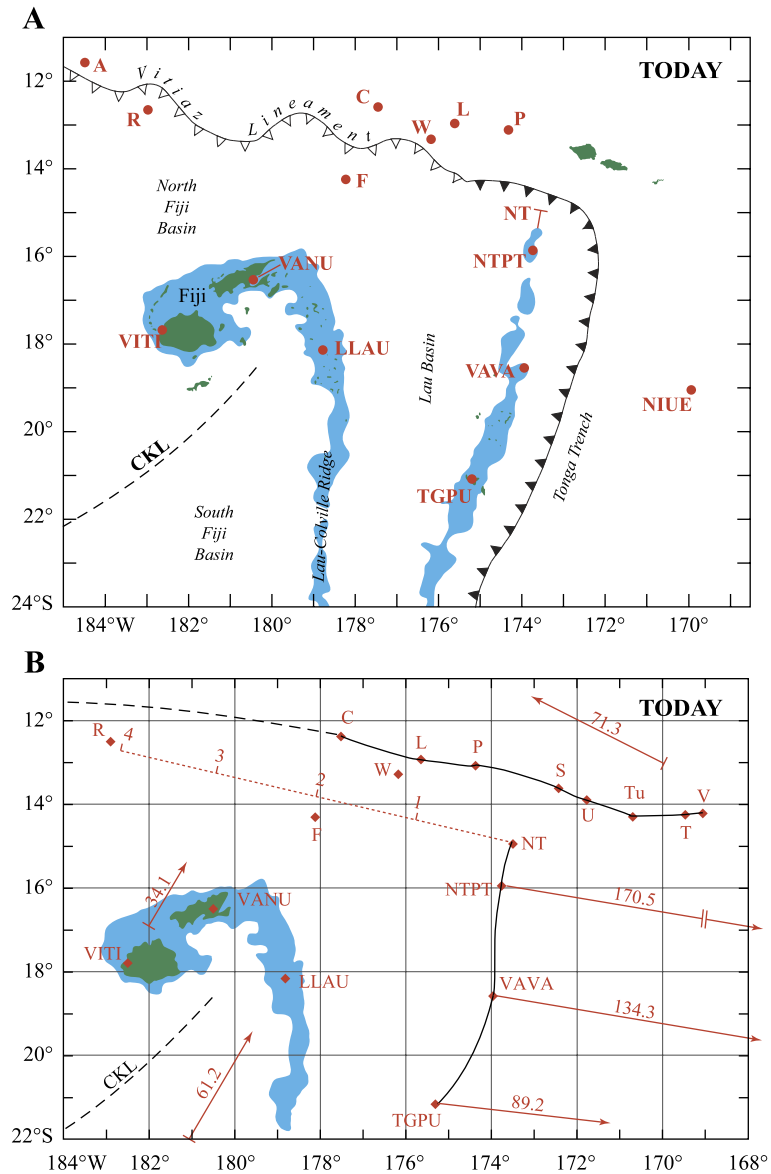
out this region [50,53,45,47], and we are left to somehow understand that the NE convergence between Fiji–Australia and the Pacific plate has been “rectified” through a series of small spreading centers, into an overall E–W divergence.

The Samoan plume center (Vailulu’u seamount [10]) has apparently migrated NE over the past 4 my, as its location now lies well north of the backtracked volcanic chain (Fig. 9D). Tutuila (Tu) was the active center at 2 my (the oldest basalts on

Tutuila are ~1.5 my [6]), and Upolu (U) was probably just becoming active at 4 my (the oldest basalts on Upolu are 2.8 my [6,11]).

6.2. Plume–trench interactions

From Fig. 9, it seems very clear that the Tonga Arc-Subduction zone likely had no impact on Samoan volcanism in the WESAM Province. Five million years ago, when Savai’i would have been



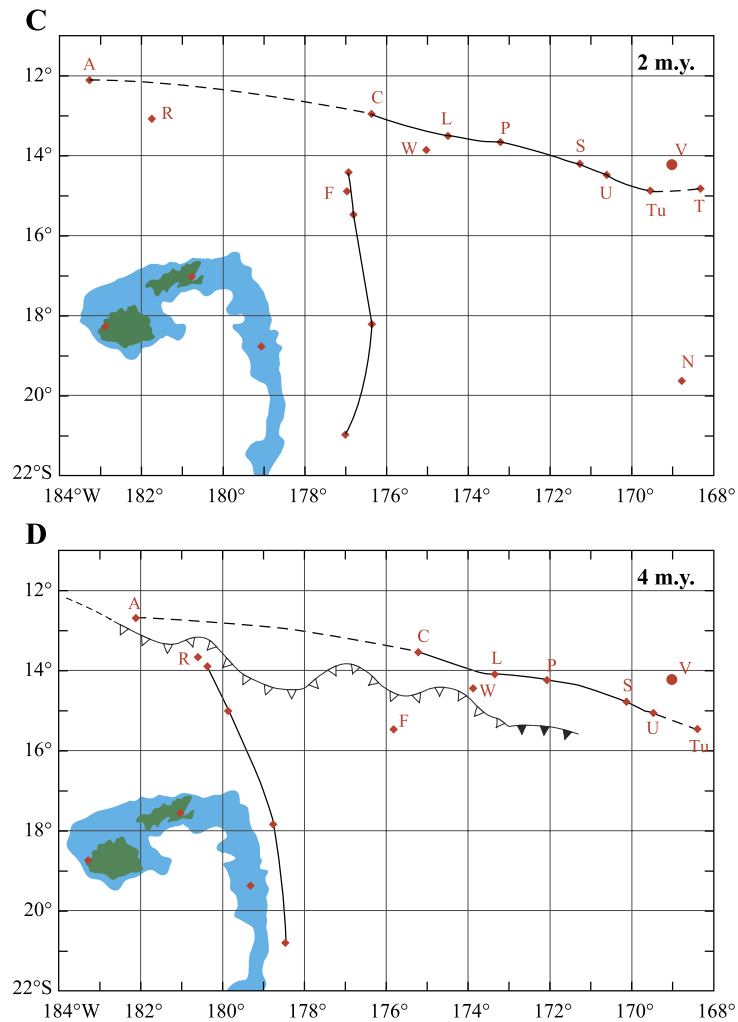


Fig. 9. Tectonic setting of the WESAM Seamounts in relation to the Fiji Plateau, Vitiiaz Lineament and the Tonga Arc (map modified from Ruellan et al. [17]). Location abbreviations: A—Alexa Bank; C—Combe Bank; F—Futuna Island; L—Lalla Rookh Bank; N—Niue Island; P—Pasco Bank; R—Rotuma Island; S—Savai'i; T—Ta'u Island; Tu—Tutuila; U—Upolu; V—Vailulu'u Seamount; CKL—Conway–Kandavu lineament (also called Hunter fracture zone; LLAU—Lakemba; NT—northern terminus, Tonga arc; NTPT—Niuatapatapu; TGPU—Tongatapu; VANU—Vanua Levu; VAVA—Vavaà; VITI—Vitu Levu. *Panel A* shows the present-day setting, with extant geodetic stations labeled; see Table 4 for derived plate motions. In *panel B*, we have connected the Tonga Arc locations and the Samoa chain features that appear to have a Samoan pedigree (Alexa Bank is assigned to the chain, but is just off the figure to the west, and connected by a dashed line). The location picked for the northern terminus of the Tonga Arc (NT) is the shallowest northernmost feature before the steep drop into the trench; a geodetic vector was derived for this location by extrapolation from the three stations further south along the arc. Futuna and Rotuma Islands, though lying to the south of the Vitiiaz Lineament, are considered to move with the Pacific Plate [48]. Vectors are shown for the present-day motions of the Pacific Plate (71.3 mm/year), the Australian Plate (61.2 mm/year) and the Fiji Plateau (34.1 mm/year), see Table 4 for references. Note that the Samoa chain does not lie along a Pacific Plate motion direction, but is more westerly; this implies a slow northward component of migration of the hotspot over the past 20 million years. The dotted line running WNW from the northern terminus of the Tonga Arc (NT) is the locus of NT positions over the past 4 million years, as they might have been registered on the Pacific Plate. *Panels C and D* show the locations of the various features at 2 and 4 my before present, as derived by backtracking the localities along the present geodetic vectors. The Vitiiaz Lineament from *panel A* has been backtracked with the Pacific Plate. Note that the northern terminus of the Tonga Arc passes Futuna Island at 2 my, and Rotuma Island at 4 my; the arc itself docks with the Lau Ridge (Fiji Plateau) at close to 4 my. Note also that the present location of the hotspot, V, is well NE of the active part of the Samoa volcanic lineament at 2 my (Tu, Tutuila) and 4 my (U, Upolu). At “Upolu Time”, the northern Tonga subduction zone was over 1200 km west of active Samoan volcanism, so is unlikely to be implicated in the volcanism.

Table 4
Geodetic plate motions in the SW Pacific

Locality	Station name	Latitude (°S)	Longitude (°W)	Velocity (mm/year)	Azimuth	Reference
Western Samoa (Faleolo, Upolu)	WSAM	13.832	172.015	71.9	N63.8W	[61]
Faleolo, W. Upolu	FALE	13.832	172.000	71.8	N63.4W	[61]
Faleolo, W. Upolu	FALE	13.83	172.00	70.2	N64.2W	[25]
Niue Island (outboard of Tonga trench)	NIUC	19.062	169.932	71.3	N62.1W	[61]
Pacific Plate average				71.3	N63.38W	
Tonga Arc, N. terminus	NT	14.95	173.50	192	E8.8S	Extrapolated
Niuatapu, N. Tonga Arc	NTPT	15.947	173.764	170.5	E8.8S	[49]
Vava'u, central Tonga Arc	VAVA	18.585	173.960	134.3	E8.8S	[49]
Tongatapu, central Tonga Arc	TGPU	21.174	175.309	89.2±0.2	E5.7S	[63]
Lakemba, Lau Ridge, Fiji	LLAU	18.167	178.817	36.1	N22.2E	[49]
Vanua Levu, Fiji (east coast)	VANU	16.50	180.50	32.6	N26.5E	[49]
Vitu Levu, Fiji (west coast)	VITI	17.80	182.50	33.7	N39.5E	[49]
Fiji average				34.1	N29.4E	
Noumea, New Caledonia	NOUM	22.270	193.590	49.9	N24.1E	[61]
Noumea, New Caledonia	NOUM	22.268	193.593	48.8	N28.9E	[62]
Noumea, New Caledonia	NOUM	22.27	193.59	48.3	N26.8E	[25]
New Caledonia average				49.0	N26.6E	
Townsville, Australia	TOW2	19.270	212.945	61.4	N28.0E	[61]
Townsville, Australia	TOW2	19.268	212.943	60.7	N30.8E	[62]
Townsville, Australia	TOW2	19.27	212.94	61.6	N29.7E	[25]
Townsville average				61.2	N29.5E	
<i>Pacific Plate locations</i>						
Vailulu'u Seamount	V	14.215	169.058			
Ta'u Island	T	14.25	169.47			
Tutuila Island	Tu	14.30	170.70			
Upolu Island (center)	U	13.90	171.77			
Savai'i Island (center)	S	13.62	172.43			
Pasco Bank (center)	P	13.08	174.37			
Lalla Rookh Seamount (center)	L	12.93	175.65			
Wallis Island	W	13.28	176.18			
Combe Seamount	C	12.38	177.52			
Futuna-Nui Island [48]	FTNA	14.31	178.12			
Rotuma Island	R	12.50	182.90			
Alexa Bank	A	11.53	184.42			

at the hotspot location, the northern terminus (NT) of the arc was more than 1400 km west of the hotspot. Combe Bank, with its age of 11 my (Table 2), had been in existence for more than 9 my when the NT passed by it ~1.8 my ago (Fig. 9C). Alexa Bank, 23 my old, was not adjacent to the NT until ~4.5 my ago (Fig. 9D). However, because of its very rapid eastward motion, the NT is quickly “closing” on the hotspot, and the voluminous rejuvenated volcanism on Savai'i may be the first witness to this interaction [1]. The apparent drift of the hotspot to the NE between 2 my and the present may also signal this interaction

(the 100 km NE migration from Tu to V in 2 my (Fig. 9C) represents a velocity of 50 mm/year).

As can be seen in Fig. 1A, the young end of the Samoan chain exhibits a series of *en echelon* lineaments, stepping off to the NE (one runs from Savai'i through the western shield on Tutuila, one runs from the eastern shield on Tutuila to Malu-malu seamount and one runs from Muli seamount through Ofu and Olosega islands to Ta'u Island; Vailulu'u appears to represent the beginning of a new lineament [11]. Assuming the hotspot is in fact “plume-driven”, then a NE motion of the plume conduit would be a natural dynamical consequence

of the eastward roll-back motion of the trench and subduction zone (and rapid opening of the Lau backarc basin). Laboratory experiments clearly show horizontal flow underneath and around the edge of a plate during roll-back, with concomitant down-flow in the mantle-wedge [54]. If there is any vertical component to this flow during escape from underneath the subducting plate, the decompression may induce minor melting that could explain some of the anomalous “off-chain” volcanism in Samoa (Uo Mamae and Papatua Seamounts, Fig. 1A). This would be an adaptation of the “adakite” model of Yogodzinski et al. [55] that posits melting whenever mantle is forced to flow around the edge of a torn subducting slab (the difference being that Uo Mamae seamount, at least, does not have “arc” chemistry [1,56,57]).

It is interesting to note that the plume motion models of Steinberger [58,59] provide some support for a NE motion for the Samoa hotspot over the past 25–30 my. These models calculate advective motions of plumes in a realistic mantle flow field, driven by surface plate motions and internal density heterogeneities inferred from seismic tomography. Fig. 10 shows the surface motion for the Samoan plume, derived for a plume initiation age of 40 my, and using

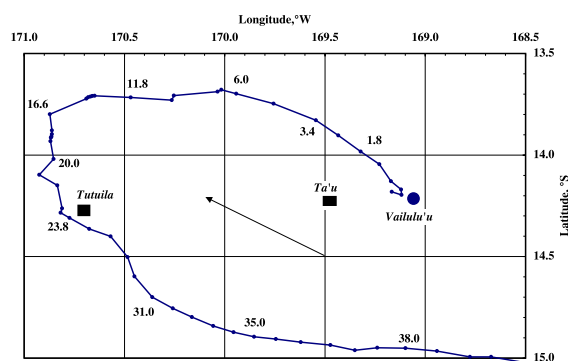


Fig. 10. Surface motion of the Samoa plume over the past 40 my, derived from a mantle dynamics model driven by surface plate motions and internal density heterogeneities. The details of this model can be found in Steinberger [59] and Steinberger et al. [60]. The initiation age assumed for the Samoan plume is 40 my; numbers at various points along the curve are ages in millions of years. The filled circle marked Vailulu'u is the present position of the plume [10]. For geographic reference, the locations of Tutuila and Ta'u Islands are also shown. The arrow marks the azimuth and distance for 1 my of present Pacific plate motion (see Table 4).

the tomographic and plate models described in [60]. The plume appears to have made a large clockwise “hook”, drifting roughly along the plate motion direction until 17 my ago, then reversing direction and drifting counter to plate motion. Overall, from 30 to 3 my, there has been a persistent NE drift of ~100 km, at a rate of about 5 mm/year.

While this motion would not explain the en echelon trends discussed above that have occurred over the past 2–3 my, it accounts for part of the misfit between the trend of the Samoa Chain and the direction of Pacific plate motion. In Fig. 9B, it is clear that the Samoan chain, as drawn from Savai'i through Pasco and Lalla Rookh to Combe, delineates a shallower azimuth (N77W) than is specified for the Pacific Plate (N63.4W; see vector marked 71.3). This misfit problem was also noted by Brocher [14]. There are several possible explanations. First, we have chosen, based on the geochemistry discussed above, to assign Pasco, Lalla Rookh and Combe a Samoan pedigree (i.e. they belong to the Samoan chain). There are other banks and seamounts in this region (e.g. Field and Horseshoe, see Fig. 1A) which might better fit the actual Pacific plate motion vector, if all were to show a Samoan pedigree. Alternatively, we have both the evidence from the dynamical plume-drift model (Fig. 10), and the en echelon arrangement of the active end of the chain, which suggest a north to northeast drift of the plume. Such a drift would generate a volcanic chain or lineament that was shallower in azimuth than the actual plate motion vector.

Resolution of this question must await both better dynamic modeling of the Samoa plume conduit (with full definition of the slab roll-back), and the isotopic characterization of all of the seamounts and banks “downstream” from the hotspot, to delimit those that are clearly Samoan and that validly may be used to define the chain. It must be recognized that several other hotspots may have left “tracks” through this region (e.g. Cook–Austral, Louisville [15–17]), and a robust geochemical fingerprinting of the myriad seamounts in this region is crucial to fully understanding the history of the Samoan hotspot.

Finally, the persistent E to SE drift shown in Fig. 10 over the past 15 my is counter to plate motion, and would have the interesting effect of increasing the “apparent” velocity of the Samoan volcanic age

progression on the Pacific Plate. This drift rate, averaged over the past 15 my, is 12 mm/year and would increase the “age progression” from 71 to 83 mm/year (creating a shallower slope in Fig. 2A, and a better fit to the Tutuila and Upolu age data).

7. Summary

- Basalts dredged from four submarine volcanic constructs west of Savai'i (Pasco, Lalla Rookh, Combe and Alexa seamounts), in the Samoan hotspot chain, are shown to have trace element and Sr, Nd and Pb isotopic signatures consistent with derivation from the Samoan hotspot.
- New $^{40}\text{Ar}/^{39}\text{Ar}$ plateau ages on Combe and Alexa basalts (11.1 and 22.9–23.9 my, respectively) fit an age progression model for Samoa, with the observed Pacific Plate velocity of 71.3 mm/year.
- A previous age for Lalla Rookh (9.8 my, Duncan [3]) also fits this age progression; we find a younger age of 1.6 my for a highly under-saturated basanite from the same dredge, suggesting a history of volcanic rejuvenation on Lalla Rookh.
- Geodetic reconstructions of the northern terminus of the Tonga arc/trench suggest that the young rejuvenated volcanism on Lalla Rookh and Savai'i may relate to interaction with the eastward migration of the trench corner (currently almost due south of Savai'i, and migrating rapidly eastward at >190 mm/year). We suggest that the Vitiaz Lineament is the trace of the eastward motion of this tear in the Pacific Plate.
- The volcanoes of the Eastern Samoan Province show an *en* echelon alignment, with the volcanic activity stepping to the northeast over the past 1–2 my. We suggest this is due to interaction of the Samoan plume with northward flow of mantle that is escaping from beneath the subducting Tonga plate, as it rolls-back to the east.

Acknowledgements

We are grateful to Jim Natland for preprints of several unpublished papers, and for his unfailing support of the anti-plume model. Matt Jackson's passion for the Samoa plume model has been a

continuous source of stimulation. Samoa is also special because of time spent in Tisa's with Hubert Staudigel and Anthony Koppers. We thank Steve Galer and Wafa Abouchami for help in implementing the Mainz Pb chemistry at WHOI. The output of high-precision Pb data from the WHOI NEPTUNE is due largely to Lary Ball's skill and tenacity; our many thanks. This research was supported by NSF EAR-0125917 (to SRH). This is SOEST contribution number 6484. We recovered from the fire of October 2002, and the coating of Pb it left in the clean labs, thanks to the unceasing help of Ernie Charette and the many other professionals at WHOI. We thank Bill White and Dave Graham for their reviews, and Hiroshi Munekane, from the Geographical Survey Institute of Japan, for the unpublished geodetic data for Tongatapu.

Appendix A. Supplementary Material

Supplementary data associated with this article can be found, in the online version, at [doi:10.1016/j.epsl.2004.08.005](https://doi.org/10.1016/j.epsl.2004.08.005).

References

- [1] J.W. Hawkins, J.H. Natland, Nephelinites and basanites of the Samoan linear volcanic chain: their possible tectonic significance, *Earth Planet. Sci. Lett.* 24 (1975) 427–439.
- [2] J. Natland, The progression of volcanism in the Samoan linear volcanic chain, *Am. J. Sci.* 280-A (1980) 709–735.
- [3] R.A. Duncan, Radiometric ages from volcanic rocks along the New Hebrides–Samoa lineament, in: T.M. Brocher (Ed.), *Investigations of the Northern Melanesian Borderland, Circum-Pacific Council for Energy and Mineral Resources Earth Science Series*, vol. 3, 1985, pp. 67–75.
- [4] J.M. Sinton, K.T.M. Johnson, R.C. Price, Petrology and geochemistry of volcanic rocks from the Northern Melanesian Borderland, in: T.M. Brocher (Ed.), *Investigations of the Northern Melanesian Borderland, Circum-Pacific Council for Energy and Mineral Resources Earth Science Series*, vol. 3, 1985, pp. 35–65.
- [5] K.T.M. Johnson, J.M. Sinton, R.C. Price, Petrology of seamounts northwest of Samoa and their relation to Samoan volcanism, *Bull. Volcanol.* 48 (1986) 225–235.
- [6] J.H. Natland, D.L. Turner, Age progression and petrological development of Samoan shield volcanoes: evidence from K–Ar ages, lava compositions and mineral studies, in: T.M. Brocher (Ed.), *Investigations of the Northern Melanesian Borderland, Circum-Pacific Council for Energy*

- and Mineral Resources Earth Science Series, vol. 3, 1985, pp. 139–172.
- [7] J.H. Natland, The Samoan Chain: A Shallow Lithospheric Fracture System, www.mantleplumes.org, 2004.
- [8] R. Montelli, G. Nolet, F.A. Dahlen, G. Masters, E.R. Engdahl, S.-H. Hung, Finite-frequency tomography reveals a variety of plumes in the mantle, *Science* 303 (2004) 338–343.
- [9] R.H. Johnson, Exploration of three submarine volcanoes in the South Pacific, *Res. Rep.-Natl. Geogr. Soc.* 16 (1984) 405–420.
- [10] S.R. Hart, H. Staudigel, A.A.P. Koppers, J. Blusztajn, E.T. Baker, R. Workman, M. Jackson, E. Hauri, M. Kurz, K. Sims, D. Fornari, A. Saal, S. Lyons, Vailulu'u undersea volcano: the new Samoa, *Geochem. Geophys. Geosyst.* GC000108 (2000) 1–13.
- [11] R.K. Workman, S.R. Hart, M. Jackson, M. Regelous, K. Farley, J. Blusztajn, M. Kurz, H. Staudigel, Recycled Metasomatized Lithosphere as the Origin of the Enriched Mantle II (EM2) End-member: evidence from the Samoan Volcanic Chain, *Geochem. Geophys. Geosyst.* 5 (2004) DOI:2003GC000623.
- [12] E. Wright, W.M. White, The origin of Samoa: new evidence from Sr, Nd and Pb isotopes, *Earth Planet. Sci. Lett.* 81 (1986/87) 151–162.
- [13] K.A. Farley, J.H. Natland, H. Craig, Binary mixing and enriched and degassed (primitive?) mantle components (He, Sr, Nd, Pb) in Samoan lavas, *Earth Planet. Sci. Lett.* 111 (1992) 193–199.
- [14] T.M. Brocher, On the age progression of the seamounts west of the Samoan islands, S.W. Pacific, in: T.M. Brocher (Ed.), *Investigations of the Northern Melanesian Borderland, Circum-Pacific Council for Energy and Mineral Resources Earth Science Series*, vol. 3, 1985, pp. 173–185.
- [15] C. Gaina, R.D. Müller, S.C. Cande, Absolute plate motion, mantle flow and volcanism at the boundary between the Pacific and Indian Ocean mantle domains since 90 Ma, in: M.A. Richards, R.G. Gordon, R.D. van de Hilst (Eds.), *The History and Dynamics of Global Plate Motions, Geophysical Monograph*, vol. 121, Am. Geophys. Union, 2000, pp. 189–210.
- [16] R.D. Müller, C. Gaina, A. Tikku, D. Mihut, S.C. Cande, J.M. Stock, Mesozoic/Cenozoic tectonic events around Australia, in: M.A. Richards, R.G. Gordon, R.D. van de Hilst (Eds.), *The History and Dynamics of Global Plate Motions, Geophysical Monograph*, vol. 121, Am. Geophys. Union, 2000, pp. 161–188.
- [17] E. Ruellan, J. Delteil, I. Wright, T. Matsumoto, From rifting to active spreading in the Lau Basin–Havre Trough backarc system (SW Pacific): locking/unlocking induced by seamount chain subduction, *Geochem. Geophys. Geosyst.* 4 (2003) GC000261.
- [18] K.T.M. Johnson, *The Petrology and Tectonic Evolution of Seamounts and Banks of the Northern Melanesian Borderland, Southwest Pacific*, Unpubl. M.Sc., University of Hawaii, 1983, 116 pp.
- [19] B.D. Taras, S.R. Hart, Geochemical evolution of the New England seamount chain: isotopic and trace element constraints, *Chem. Geol.* 64 (1987) 35–54.
- [20] S.J.H. Galer, *Chemical and isotopic studies of crust–mantle differentiation and the generation of mantle heterogeneity*, Unpubl. PhD, University of Cambridge, 1986.
- [21] W. Abouchami, S.J.G. Galer, A. Koschinsky, Pb and Nd isotopes in NE Atlantic Fe–Mn crusts: proxies for trace metal paleosources and paleocean circulation, *Geochim. Cosmochim. Acta* 63 (1999) 1489–1505.
- [22] S.R. Hart, R.K. Workman, M. Coetzee, J. Blusztajn, L. Ball, K.T.M. Johnson, The Pb isotope pedigree of Western Samoan volcanics: new insights from high-precision analysis by NEPTUNE ICP/MS, *EOS* 83 (2002) F20.
- [23] W. Todt, R.A. Cliff, A. Hanser, A.W. Hofmann, Evaluation of a ^{202}Pb – ^{205}Pb double spike for high-precision lead isotope analysis, in: A. Basu, S.R. Hart (Eds.), *Earth Processes: Reading the Isotopic Code, Geophysical Monograph*, vol. 95, 1996, pp. 429–437.
- [24] I. McDougall, Age and evolution of the volcanoes of Tutuila, American Samoa, *Pac. Sci.* 39 (1987) 311–320.
- [25] G.F. Sella, T.H. Dixon, A. Mao, I. REVEL: a model for recent plate velocities from space geodesy, *J. Geophys. Res.* 107 (ETG 11) (2002) 1–32.
- [26] R.C. Price, L.E. Johnson, A.J. Crawford, Basalts of the North Fiji Basin: the generation of back arc basin magmas by mixing of depleted and enriched mantle sources, *Contrib. Mineral. Petrol.* 105 (1990) 106–121.
- [27] S.R. Hart, K, Rb, Cs contents and K/Rb, K/Cs ratios of fresh and altered submarine basalts, *Earth Planet. Sci. Lett.* 6 (1969) 295–303.
- [28] A.W. Hofmann, W.M. White, Ba, Rb, Cs in the Earth's mantle, *Z. Naturforsch.* 38a (1983) 256–266.
- [29] J.A. Philpotts, C.C. Schnetzler, S.R. Hart, Submarine basalts: some K, Rb, Sr, Ba, rare earth, H₂O and CO₂ data bearing on their alteration, modification by plagioclase, and possible source materials, *Earth Planet. Sci. Lett.* 7 (1969) 293–299.
- [30] M.D. Feigenson, A.W. Hofmann, F.J. Spera, Case studies on the origin of basalt: II. The transition from tholeiitic to alkalic volcanism on Kohala volcano, Hawaii, *Contrib. Mineral. Petrol.* 84 (1983) 390–405.
- [31] S.R. Hart, H. Staudigel, Isotopic characterization and identification of recycled components, 15–28, in: S.R. Hart, L. Gulen (Eds.), *Crust/Mantle Recycling at Convergence Zones, NATO ASI Series C*, vol. 258, Kluwer Academic Publishers, Dordrecht, The Netherlands, 1989.
- [32] G.A. Macdonald, T. Katsura, Chemical composition of the Hawaiian lavas, *J. Petrol.* 5 (1964) 83–133.
- [33] M. LeBas, R.W. Maitre, A. Streckeisen, B. Zanettin, A chemical classification of volcanic rocks based on the total alkali–silica diagram, *J. Petrol.* 27 (1986) 745–750.
- [34] A. Zindler, S.R. Hart, Chemical geodynamics, *Annu. Rev. Earth Planet. Sci.* 14 (1986) 493–571.
- [35] S.R. Hart, A large-scale isotopic anomaly in the southern hemisphere mantle, *Nature* 309 (1984) 753–757.

- [36] J.D. Woodhead, C.W. Devey, Geochemistry of the Pitcairn seamounts: I. Source character and temporal trends, *Earth Planet. Sci. Lett.* 116 (1993) 81–99.
- [37] J. Eisele, M. Sharma, S.J.G. Galer, J. Blichert-Toft, C.W. Devey, A.W. Hofmann, The role of sediment recycling in EM-I inferred from Os, Pb, Hf, Nd, Sr isotope and trace element systematics of the Pitcairn hotspot, *Earth Planet. Sci. Lett.* 196 (2002) 197–212.
- [38] Hart, Hauri and Farley, unpublished.
- [39] J.D. Woodhead, Extreme HIMU in an oceanic setting: the geochemistry of Mangaia Island (Polynesia), and temporal evolution of the Cook–Austral hotspot, *J. Volcanol. Geoth. Res.* 72 (1996) 1–19.
- [40] E.H. Hauri, S.R. Hart, Re–Os isotope systematics of HIMU and EMII oceanic island basalts from the south Pacific Ocean, *Earth Planet. Sci. Lett.* 114 (1993) 353–371.
- [41] E.H. Hauri, S.R. Hart, Rhenium abundances and systematics in oceanic basalts, *Chem. Geol.* 139 (1997) 185–205.
- [42] A.W. Hofmann, Chemical differentiation of the Earth: the relationship between mantle, continental crust and oceanic crust, *Earth Planet. Sci. Lett.* 90 (1988) 297–314.
- [43] W.F. McDonough, S.S. Sun, The composition of the earth, *Chem. Geol.* 120 (1995) 223–253.
- [44] C.Y. Yan, L.W. Kroenke, A plate tectonic reconstruction of the Southwest Pacific, 0–100 Ma, in: W.H. Berger, L.W. Kroenke, L.A. Mayer, et al. (Eds.), *Proceedings of the Ocean Drilling Program. Scientific Results*, vol. 130, 1993, pp. 697–709.
- [45] B. Pelletier, S. Calmant, R. Pillot, Current tectonics of the Tonga–New Hebrides region, *Earth Planet. Sci. Lett.* 164 (1998) 263–276.
- [46] C. DeMets, R.G. Gordon, D.F. Argus, S. Stein, Effect of recent revisions to the geomagnetic reversal time scale on estimates of current plate motions, *Geophys. Res. Lett.* 21 (1994) 2191–2194.
- [47] K.E. Zellmer, B. Taylor, A three-plate kinematic model for Lau Basin opening, *Geochem. Geophys. Geosyst.* 2 (2001) DOI:2000GC000106.
- [48] S. Calmant, B. Pelletier, P. Lebellegard, M. Bevis, F.W. Taylor, D.A. Phillips, New insights on the tectonics along the New Hebrides subduction zone based on GPS results, *J. Geophys. Res.* 108 (2003) 1–22 (ETG 17).
- [49] M. Bevis, F.W. Taylor, B.E. Schutz, J. Recy, B.L. Isacks, S. Helu, R. Singh, E. Kendrick, J. Stowell, B. Taylor, S. Calmant, Geodetic observations of very rapid convergence and back-arc extension at the Tonga arc, *Nature* 374 (1995) 249–251.
- [50] J.W. Hawkins, Evolution of the Lau Basin: insights from ODP 135, in: B. Taylor, J. Natland (Eds.), *Active Margins and Marginal Basins of the Western Pacific*, *Geophys. Monog. Ser.*, AGU, Washington, DC, 1995, pp. 125–173.
- [51] T.M. Brocher, On the formation of the Vitiaz trench lineament and North Fiji basin, in: T.M. Brocher (Ed.), *Investigations of the Northern Melanesian Borderland*, Circum-Pacific Council for Energy and Mineral Resources Earth Science Series, vol. 3, 1985, pp. 13–33.
- [52] D.W. Millen, M.W. Hamburger, Seismological evidence for tearing of the Pacific plate at the northern termination of the Tonga subduction zone, *Geology* 26 (1998) 659–662.
- [53] B. Pelletier, Y. Lagabreille, M. Menoît, G. Cabioch, S. Calmant, E. Garel, C. Guivel, J. Perrier, Newly discovered active spreading centers along the North Fiji transform zone (Pacific–Australia Plate boundary): preliminary results of the R/V l’Atalante Alaufi Cruise (February–March 2000), *Ridge Events*, 2001, pp. 7–9 Feb.
- [54] C. Kincaid, R.W. Griffiths, Laboratory models of the thermal evolution of the mantle during rollback subduction, *Nature* 425 (2003) 58–62.
- [55] G.M. Yogodzinski, J.M. Lees, T.G. Churikova, F. Dorendorf, G. Wöerner, O.N. Volynets, Geochemical evidence for the melting of subducting oceanic lithosphere at plate edges, *Nature* 409 (2001) 500–504.
- [56] A.Y. Sharaskin, I.K. Pustchin, S.K. Zlobin, G.M. Kolesov, Two ophiolite sequences from the basement of the Northern Tonga arc, *Ofioliti* 8 (1983) 411–430.
- [57] S.K. Zlobin, G.M. Kolesov, N.N. Kononkova, Development of within-plate magmatism on the landward and offshore slopes of the Tonga Trench, *Ofioliti* 16 (1991) 17–35.
- [58] B. Steinberger, Plumes in a convecting mantle: models and observations for individual hotspots, *J. Geophys. Res.* 105 (2000) 11127–11152.
- [59] B. Steinberger, Motion of the Easter hot spot relative to Hawaii and Louisville hotspots, *G-Cubed* 3 (2002) GC000334.
- [60] B. Steinberger, R. Sutherland, R.J. O’Connell, Prediction of Emperor–Hawaii seamount locations from a revised model of plate motion and mantle flow, *Nature* 430 (2004) 167–173.
- [61] J. Bevan, P. Tregoning, M. Bevis, T. Kato, C. Meertens, Motion and rigidity of the Pacific Plate and implications for plate boundary deformation, *J. Geophys. Res.* 107 (2002) 1–15 (ETG 19).
- [62] P. Tregoning, Plate kinematics in the western Pacific derived from geodetic observations, *J. Geophys. Res.* 107 (2002) 1–8 ECV 7.
- [63] H. Munekane, Geographical Survey Institute of Japan, personal communication, June 2004.
- [64] S.R. Hart, R.K. Workman, L. Ball, J. Blusztajn, High Precision Pb Isotope Techniques from the WHOI NEPTUNE PIMMS WHOI Plasma Facility Open File Technical Report, 10, 2004 <http://www.whoi.edu/science/GG/people/shart/Open_File/open_file.htm>.
- [65] C. Class, S.L. Goldstein, Plume–lithosphere interactions in the ocean basins: constraints from the source mineralogy, *Earth Planet. Sci. Lett.* 150 (1997) 245–260.